Estimation of Cross-Tropopause Airmass Fluxes at Midlatitudes: Comparison of Different Numerical Methods and Meteorological Situations

J. KOWOL-SANTEN,* H. ELBERN, AND A. EBEL

Institute for Geophysics and Meteorology, University of Cologne, Cologne, Germany

(Manuscript received 2 June 1999, in final form 18 April 2000)

ABSTRACT

Airmass flux across the tropopause modifies the budget of chemically reactive minor constituents in the stratosphere and the troposphere. Flux estimates reported in the literature exhibit large discrepancies, mainly due to the application of different estimation algorithms and examination of different episodes. The different studies also focus on different exchange mechanisms. With the aim of contributing to clarification of the situation, two different methods of cross-tropopause mass transfer calculations are implemented into the mesoscale-α European Air Pollution Dispersion model system and discussed: a trajectory-based analysis and the method developed by Wei. These methods are applied to an episode in February 1997, when a deep stratospheric intrusion occurred over the North Atlantic and western Europe. Comparison of the results shows good agreement between the net flux values computed by the different methods, both yielding values near 1×10^{-3} kg m^{-2} s^{-1} for the net airmass flux from the stratosphere to the troposphere. Analyzing the tendency of potential vorticity along trajectories, it is shown that in this case turbulent processes surpass the diabatic ones and are mainly responsible for the transformation from stratospheric into tropospheric air. Employing the method of trajectory analysis, different meteorological situations are investigated in order to establish a broader range of cross-tropopause transport estimates for middle latitudes. For all analyzed cases a net downward transport from stratosphere to troposphere was found. The results vary between 0.6 and 1.0×10^{-3} kg m^{-2} s^{-1} for the airmass flux across the two potential vorticity unit surface, taken as the dynamical tropopause.

1. Introduction

In order to explain the variability of chemical species in the troposphere as well as in the stratosphere, it is necessary to understand the dynamical processes at the tropopause and to estimate the amount of their exchange between the stratospheric and the tropospheric reservoirs.

Though various studies have been carried out to quantify the cross-tropopause airmass and ozone flux at middle latitudes on the planetary scale (e.g., Hoerling et al. 1993; Grewe and Dameris 1996; Gettelman and Sobel 2000) and on the mesoscale (e.g., Ancellet et al. 1991; Ebel et al. 1991, 1996; Lamarque and Hess 1994; Spaete et al. 1994; Vaughan et al. 1994), the results show considerable scatter between 12 and 137×10^{10} molecules cm^{-2} s^{-1} for the ozone fluxes and 0.5 and 3.5×10^{-3} kg m^{-2} s^{-1} for airmass fluxes, respectively. Many factors are responsible for these different results. Of course, one of the most important is the variability of the considered meteorological situations. So far the studies often treat only a single event; comparative studies are rare. Moreover, the methods applied are different.

Lamarque and Hess (1994), Ebel et al. (1996), and Wirth and Egger (1999), for instance, applied the diagnostic formula of Wei (1987) on the mesoscale. Grewe and Dameris (1996) and Gettelman and Sobel (2000) used the same method working with coarser global datasets. A direct comparison between these results is limited by the following points: (i) analysis of different time periods, (ii) the use of different models, and (iii) different scales and the different vertical and horizontal resolutions of the models.

Ancellet et al. (1991) and Vaughan et al. (1994) used ozone measurements and trajectories based on the European Centre for Medium-Range Weather Forecasts (ECMWF) analyses to quantify the amount of air and ozone transported from the stratosphere into the troposphere. The problem they discussed is the coarse horizontal resolution of this technique, which leads to an error estimate of 50% (Ancellet et al. 1991).

Another reason that makes a direct comparison of the published estimates difficult is the different representation of transfer rates. While in a variety of studies the

* Current affiliation: Service d'Aéronomie du CNRS, Paris, France.

Corresponding author address: Dr. Johanna Kowol-Santen, Service d'Aéronomie du CNRS, Université Pierre et Marie Curie, Tour 15-Couloir 15-14 4, Place Jussieu, 75232 Paris Cedex 05, France.
E-mail: kowol@aero.jussieu.fr

transfer rates of ozone are calculated (e.g., Ancellet et al. 1991; Ebel et al. 1991) there are also several purely dynamically based approaches providing airmass fluxes (e.g., Spaete et al. 1994; Vaughan et al. 1994). In addition some authors, for example, Lamarque and Hess (1994) and Ebel et al. (1996), derive ozone transfer from airmass fluxes by assuming a linear relationship between ozone and potential vorticity (PV) close to the tropopause.

One of the often discussed and still not entirely clarified questions concerns the mechanisms for the change in potential vorticity and therefore irreversible transport across the tropopause. Lamarque and Hess (1994) and Wirth (1995) discuss the role of diabatic effects as the most important process modifying the PV budget. By contrast Shapiro (1980) and Price and Vaughan (1993) show case studies where turbulent diffusion surpassed diabatic process. These studies have mainly been performed using rather an idealized balanced vortex model (Wirth 1995) or analyzing again a single event (Lamarque and Hess 1994; Shapiro 1980).

In a recent work Wirth and Egger (1999) compared different methods of diagnosing the synoptic-scale mass exchange. The calculations were based on a T106 ECMWF model run with 31 vertical levels and a temporal resolution of 3 h. The authors discuss strong numerical artifacts when applying Wei's formula.

Fluxes across the tropopause are not directly measurable. The quality of a simulation-based assessment of fluxes depends on both the meteorological model and the ensuing flux algorithm. In a preceding paper, Ravetta et al. (1999) could establish confidence in the mesoscale model's performance in resolving tropopause folds. The validation of meteorological parameters (potential temperature and wind) as well as the comparison between the temporal evolution of measured ozone mixing ratio and modeled PV distribution revealed a very good agreement between measurements and results of mesoscale simulations. The focus here is placed on the further question of the pertinent flux estimate method.

In order to achieve more reliable estimates of the amount of air mass transported across the tropopause it is advantageous to analyze various meteorological situations applying the same method.

The first aim of this study is to synthesize and compare results obtained with two different methods in order to quantify the exchange across the tropopause, that is, the formulation of Wei and trajectory analysis. Using both methods a case study in February 1997 is analyzed. The second aim is the quantification of transport across the tropopause for different meteorological situations applying one method. The estimations have been done using the European Air Pollution Dispersion (EURAD) model system, which is designed for mesoscale chemistry transport simulations driven by the Pennsylvania State University–National Center for Atmospheric Research (Penn State–NCAR) fifth-generation Mesoscale Model (MM5).

The paper is organized as follows. In section 2 we present the EURAD model system and the methods applied for the flux estimates across the tropopause. In section 3 we compare the two analyzing methods for a single meteorological situation. The exchange estimates calculated via the trajectory method for different meteorological situations are discussed in section 4. Finally, conclusions are given in section 5.

2. Model system and methodology

a. The EURAD model system

The EURAD model is a system of simulation tools which handle transport, diffusion, and chemical transformation of trace species on the mesoscale α. The main parts are the Penn State–NCAR MM5 and the Chemistry Transport Model (Fig. 1). MM5 is an Eulerian primitive equation model with a selected integration domain. For initial and boundary conditions ECMWF T106 analyzes are used. Key parameterizations for the simulation of airmass transport include the Blackadar (1979) mixing layer scheme, *K* theory of vertical diffusion with Richardson number dependent coefficient K_z, fourth-order horizontal diffusion in the interior of the model domain and second-order form at the lateral boundaries, and a Kuo (1974) cumulus parameterization. A comprehensive description of the model design is given by Grell et al. (1993). We used the hydrostatic mode option of MM5, as the focus is placed on upper-tropospheric dynamics with a horizontal resolution of 50 km. Studies carried out by Kowol-Santen (1998) and Ravetta et al. (1999) have shown that a horizontal resolution ranging between 40 and 50 km is suitable to simulate the tropopause dynamics. The horizontally staggered grid for the prognostic variables surface pressure, temperature, water vapor, and horizontal wind velocity is based on the Arakawa B-grid scheme. For the purpose of simulating tropopause dynamics the vertical structure was adapted by extension of the upper lid of the model domain up to 10 hPa and refinement of the vertical resolution in the lower stratosphere and upper troposphere (Ebel et al. 1996; Elbern et al. 1997). The present study is based on a 110 $\times$ 80 grid centered at 50°N and 20°W (e.g., Fig. 4). The number of vertical levels is 29 with an average spacing of 30 hPa in the free and upper troposphere and the lower stratosphere between 500 and 10 hPa.

Several validation studies have been carried out (e.g., Elbern et al. 1997; Kowol-Santen 1998; Ravetta et al. 1999) that prove the applicability of the EURAD model system for the simulation of dynamics of the tropopause region.

b. Methodology

Two methods were applied for the estimation of cross-tropopause transport for a case study in February 1997.

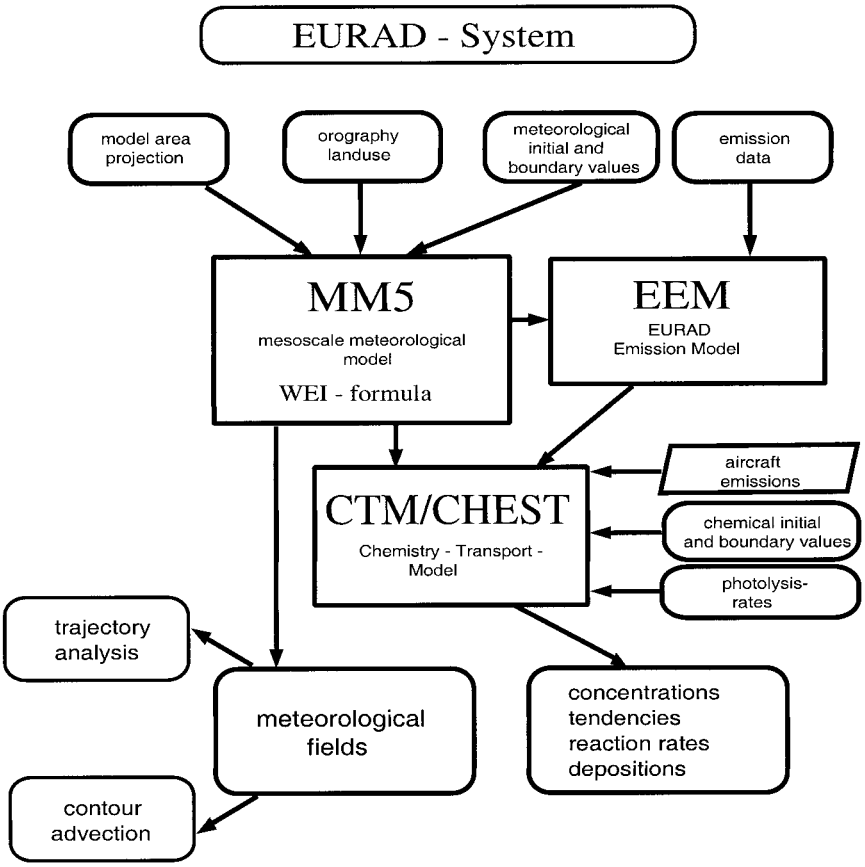

FIG. 1. Scheme of the EURAD model system.

An algorithm based on trajectory analyzes has been developed specifically for this study. As a second method the formula of Wei (Wei 1987) was implemented in the EURAD model system. For all these studies the tropopause is defined to coincide with the 2-PVU surface, where a potential vorticity unit (PVU) is given by 1×10^{-7} K Pa^{-1} s^{-1}.

1) TRAJECTORY ANALYSIS

In order to follow the movement of air parcels and to quantify the exchange of matter, an algorithm based on trajectory analyzes was developed and applied. In the EURAD model system trajectories are calculated using the three-dimensional wind fields of MM5 with a temporal resolution of 1 h. The parcels' positions are updated every 10 min by interpolating the modeled winds and advecting the parcels with a two-step iteration in three dimensions.

For the quantitative estimates of stratosphere–troposphere exchange the analyzed area (in this case an upper-level trough) is embedded in a three-dimensional box enclosing the upper troposphere and lower stratosphere (Fig. 2). The vertical and horizontal extension of the box is determined by the structure of the 2-PVU surface (i.e., the tropopause) as calculated from MM5 results. The box covers the area where the tropopause is situated below 250 hPa in the region of the analyzed dynamical feature (Fig. 2). Forward trajectories are started every 6 h from each grid point inside the box. In the case under investigation one has 60×35 grid boxes in the horizontal ($\sim 5.25 \times 10^6$ km^2) and 10 isobaric surfaces between 250 and 475 hPa in the vertical inside the box. In this way 21 000 trajectories are released every 6 h. An initial mass is assigned to each parcel or air volume using density and geopotential height of the isobaric surfaces as derived by the MM5. The mass is assumed to remain constant within the analyzed time interval. The calculation of large ensembles of trajectories together with high vertical and horizontal resolution helps to avoid the problem of changing particle sizes caused, for example, by strong dilution or accumulation of particles in certain areas. During the analyzed episode the vertical and horizontal extension of the box follows the variation of the trough's size and position (Fig. 2). The number of trajectory release points is kept constant. Along each trajectory the evolution of potential vorticity is determined from the interpolated model value and compared to a threshold value defining the tropopause level. The mass of air transported from the troposphere

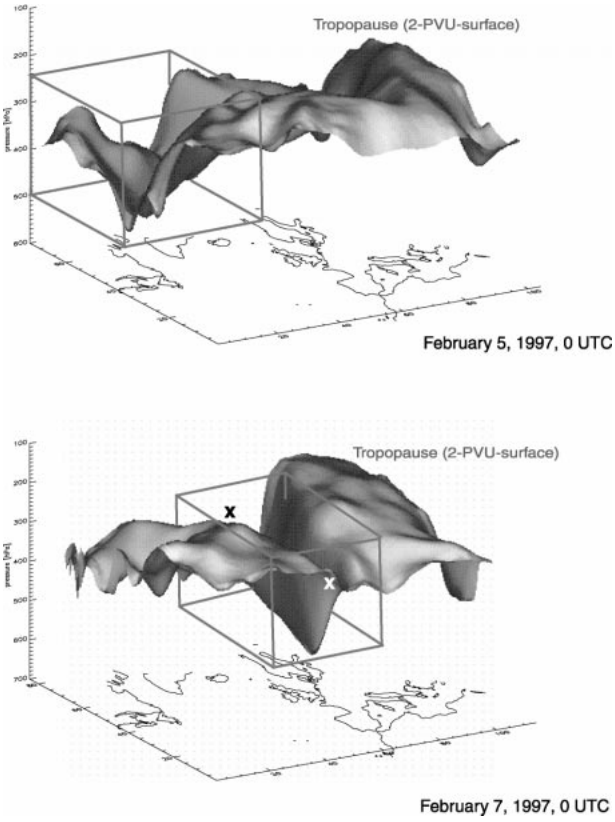

FIG. 2. Three-dimensional view of the dynamical tropopause (2-PVU surface) at 0000 UTC 5 and 7 Feb 1997. The boxes mark the regions of particle release for the cross-tropopause airmass transport estimates (see text).

to the stratosphere (in the following indicated by positive values) is estimated by summing up the mass of the parcels that revealed an increase in PV within the analyzed time period (e.g., 6 h) surpassing the threshold value. Conversely, the amount of air transported from the stratosphere to the troposphere (in the following indicated by negative values) is estimated by summing up the mass of the parcels that revealed a decrease of PV below the threshold value. Sensitivity studies carried out with time intervals of 12 and 24 h show larger differences (of up to 20%) between the upward and downward fluxes while the net fluxes show differences of less than 5%. Moreover, the application of larger time intervals sometimes involves the problem of multiple crossings of the tropopause, which becomes negligible (less than 5% of the trajectories) when looking at time periods equal or shorter than 6 h.

In order to achieve a better understanding of the physical processes modifying the PV budget, a tendency analysis is carried out. As potential vorticity is not a prognostic variable of the MM5, we determine the PV tendency by calculating the temporal change of the prognostic variables temperature (T), pressure (p), and horizontal wind ($\mathbf{u}$). Following Pedlosky (1979) and Lamarque and Hess (1994), the temporal change of potential vorticity is given by

$$\frac{\partial \mathrm{PV}}{\partial t} = \frac{\partial}{\partial t}\left(\frac{1}{\rho}(\boldsymbol{\nabla} \times \mathbf{u} + f\mathbf{k}) \cdot \boldsymbol{\nabla}\theta\right)$$
$$= \frac{1}{\rho}\left(\boldsymbol{\nabla} \times \frac{\partial \mathbf{u}}{\partial t}\right) \cdot \boldsymbol{\nabla}\theta + \frac{1}{\rho}(\boldsymbol{\nabla} \times \mathbf{u} + f\mathbf{k}) \cdot \boldsymbol{\nabla}\left(\frac{\partial \theta}{\partial t}\right)$$
$$- \frac{\mathrm{PV}}{\rho}\left(\frac{1}{RT}\frac{\partial p}{\partial t} - \frac{p}{RT^2}\frac{\partial T}{\partial t}\right), \quad (1)$$

where θ denotes the potential temperature, f the Coriolis parameter, ρ the density, and R the ideal gas constant. The processes contributing to the temporal change of the horizontal wind components are advection, diffusion, and the pressure gradient. The temperature changes are due to advection, diffusion, radiation, and cloud effects.

This analysis allows for explicitly distinguishing between the contribution of the diabatic and the turbulent diffusive processes to the change of the PV budget along the trajectories.

2) THE METHOD OF WEI

Based on the equation of continuity Wei (1987) proposed a formula for local flux estimate from the Eulerian point of view. The airmass flux perpendicular to the tropopause is given by

$$F(\rho) = \left[\rho J_\theta\left(\frac{d\theta}{dt} - \frac{\partial \theta_{\mathrm{TP}}}{\partial t} - \mathbf{u} \cdot \boldsymbol{\nabla}_\theta \theta_{\mathrm{TP}}\right)\right]_{\theta_{\mathrm{TP}}}, \quad (2)$$

where θ_{TP} is the potential temperature at the tropopause (2-PVU surface) and J_θ is the Jacobi matrix of the transformation from the (x, y, z) to (x, y, θ) system. It takes into account the vertical velocity at the tropopause, the local vertical change of the tropopause position, and the isentropic transport across the tropopause. A particularly simple form is attained if the potential vorticity is taken as the vertical coordinate (Hoerling et al. 1993):

$$F(\rho) = \rho \frac{\partial z}{\partial \mathrm{PV}} \frac{d\mathrm{PV}}{dt}. \quad (3)$$

In their diagnostic study based on global T106 ECMWF analyses, Wirth and Egger (1999) reported best results when using the latter formulation due to its lack of noise. For high-resolution model output as produced by MM5 simulations PV is not an option for a vertical coordinate as it does not provide a one-to-one mapping on geometric height everywhere. As is shown later (Fig. 6), $\partial z/\partial \mathrm{PV}$ is no longer finite and even reverses sign at the most sensitive locations of a tropopause fold. We therefore implemented (2) and filtered noise by averaging temporal differentiation over 1 h.

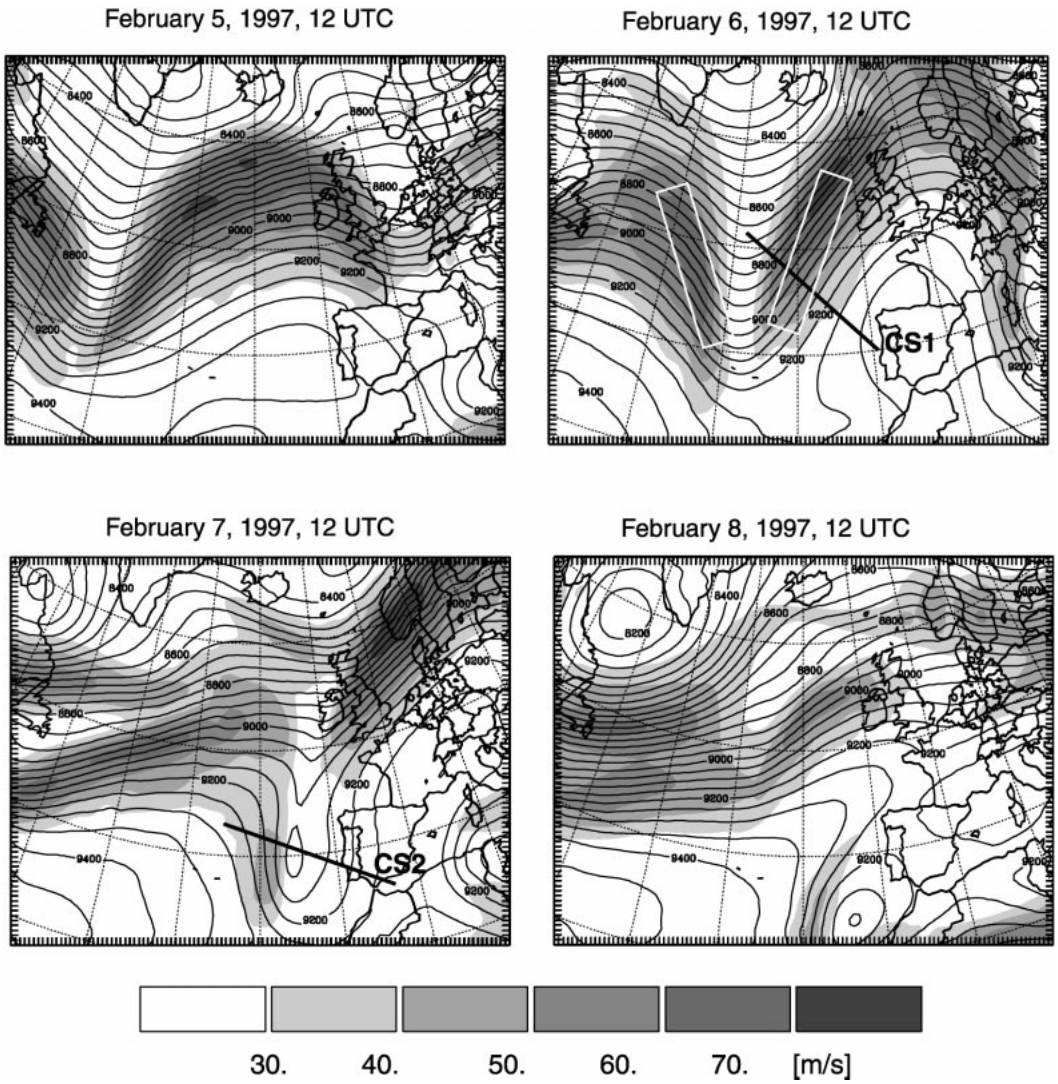

FIG. 3. Geopotential height (isolines) and horizontal wind (gray shading) for the 300-hPa surface from 1200 UTC 5 Feb to 1200 UTC 8 Feb 1997. The white boxes mark the positions of the trajectories discussed in the text. For information on lines CS1 and CS2 see Fig. 6.

3. Case study: February 1997

The numerical simulations were initialized at 0000 UTC 1 February 1997 and run for a time period of 8 days (as described in section 2a). The meteorological situation under investigation is characterized by high meridional pressure gradients. An upper-level trough is moving from Greenland eastward over the North Atlantic and expanding southward during the first days of February. Figure 3 shows a time sequence of horizontal wind and geopotential height on the 300-hPa surface from 1200 UTC 5 February to 1200 UTC 8 February as calculated with the MM5. The model results show a maximum wind speed of 70 m s^{-1} on 5 February, which extends southward. The trough deepens on the following day and becomes elongated with a pronounced north–south axis.

The spatial and temporal evolution of the meteorological situation is also evident from the potential vorticity maps as depicted in Fig. 4 at the 320-K isentropic surface from 1200 UTC 6 Feb to 0000 UTC 8 February. In the evening hours of 7 February the tip of the filament starts to roll up near the west coast of Portugal and evolves to a distinct vortex during the following hours. The state after the modeled thinning of the through with ensuing development of a filament and rolling up to a coherent and isolated structure is also exhibited in the Meteosat water vapor images. As an example Fig. 5 shows the *Meteosat-4* infrared cloud image at 1200 UTC 8 February 1997. On 8 February the streamer breaks up under the influence of the large-scale deformation field.

Meanwhile, the surface cyclone moves from Iceland toward Scandinavia while the associated frontal zone

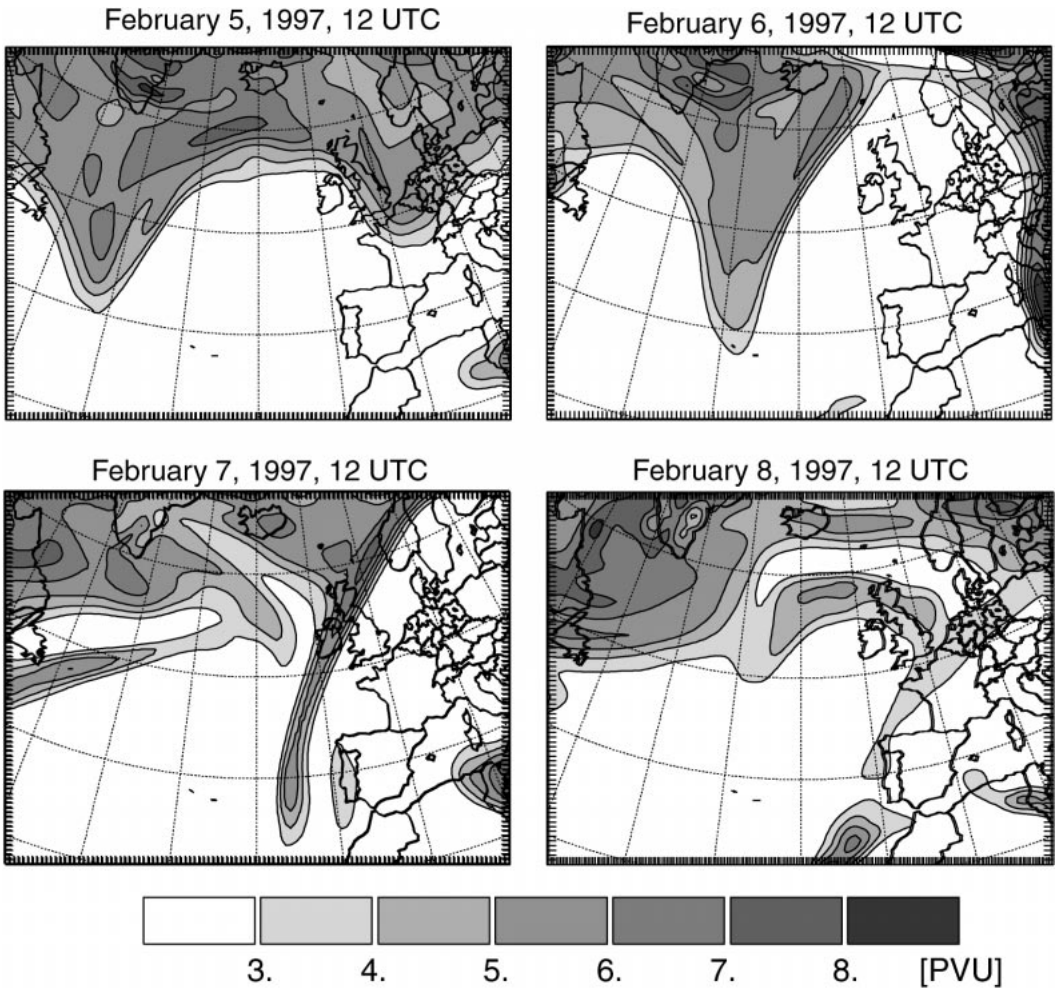

FIG. 4. Development of the PV field on the 320-K isentropic surface from 1200 UTC 5 Feb to 1200 UTC 8 Feb.

crosses the North Atlantic toward central Europe. Figure 6 shows two vertical cross sections of potential temperature and the 2-PVU surface across the eastern flank of the trough at 1200 UTC 6 February and across the southern part of the developing streamer at 1200 UTC 7 February (as marked by the lines CS1 and CS2 in Fig. 3). The upper-level frontogenesis associated with the jet streak leads to an enfolding of the tropopause whereby the tip of the fold intrudes to 550 hPa on 6 February and farther down to 650 hPa on the following day.

a. Results of the trajectory analysis

To study the transport processes in the vicinity of the trough and the developing streamer, the trajectory algorithm was applied with 21 000 forward trajectories as described in section 2b. The parcels were released every 6 h from 0000 UTC 5 February to 0000 UTC 8 February (Fig. 2). The results of this analysis show three main types of parcel displacement. Trajectories released at the western and eastern flanks of the trough (as indicated by the white boxes in Fig. 3) reveal subsidence into the free troposphere between the trough and the neighboring upper-level ridges over the Atlantic and western Europe (Fig. 3). The deep tropopause fold on 7 February (Figs. 2 and 6) was coupled to a cold front that moved eastward. Due to strong downward winds at the front, parcels initialized in the lower northern part of the fold are transported deep into the free and lower troposphere (500–800 hPa). A different result was obtained for trajectories released in the eastern part of the fold above 350 hPa, where an upward transport of tropospheric air parcels into the stratosphere occurs. In addition a tendency analysis was carried out along the trajectories (see previous section) in order to achieve a better understanding of the processes impinging upon the potential vorticity. For the sake of brevity we only discuss two typical trajectories in detail.

The first trajectory considered here was started at 300 hPa at 0000 UTC 7 February in the northern part of the fold (black cross in Fig. 2). The horizontal and vertical displacement of this air parcel during the following 24

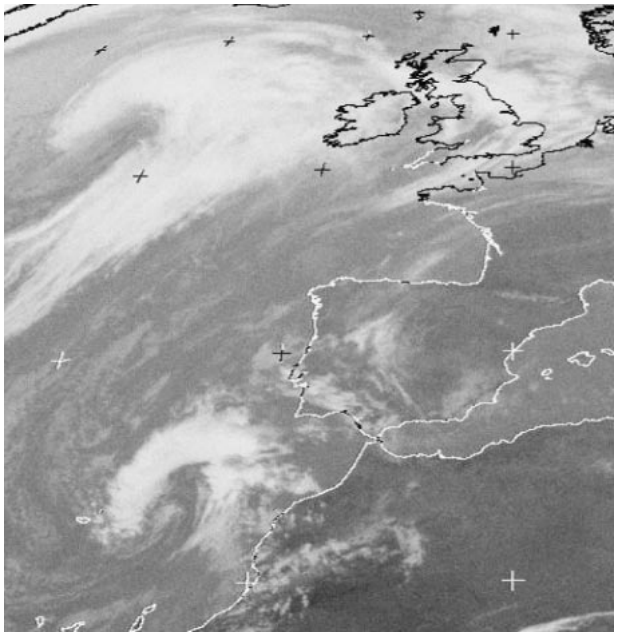

FIG. 5. *Meteosat-4* infrared cloud image at 1200 8 Feb 1997.

h is shown in the upper and middle panels of Fig. 7, respectively. During the first 7 h when the parcel moves southeast and subsides down to 400 hPa the potential vorticity remains almost constant at 3.5 PVU. In the following 8 h the potential vorticity decreases to 1.7 PVU while the air parcel moves farther to the south and down to 550 hPa. During the same time period a slight decrease in potential temperature of -0.7K $(8\ \text{h})^{-1}$ can be observed. The results of the tendency analysis show that in this particular case the temporal change of the vertical gradient of potential temperature plays a minor role in the transport across the tropopause as compared to diffusive processes. Figure 8 displays a cross section of the 2-PVU surface and of the potential vorticity tendency due to diffusion at 0900 UTC 7 February along 46°N. At this time the trajectory (marked by a black cross in Fig. 8) is at 400 hPa, well inside the stratosphere, but the whole area of the enfolded tropopause between 300 and 530 hPa shows a negative tendency of potential vorticity due to turbulent diffusion. The model output exhibits very low Richardson numbers inside the fold due to strong vertical wind shear at the steep frontal zone. Compared to the influence of turbulent diffusion, diabatic effects are of minor importance as they only contribute 1% of the total amount.

The second trajectory was initialized at 275 hPa at 0000 UTC 7 February in the southern part of the tropopause fold (white cross in Fig. 2). While the air parcel moves northward and subsides by nearly 10 hPa during the first 6 h, the potential vorticity stays constant (1.1 PVU). Compared to the previous trajectory the vertical displacement is very small in this case (25 hPa in comparison to 250 hPa). After 0700 UTC the parcel rises and the potential vorticity increases reaching a maximum of 2.4 PVU on at 0000 UTC 8 February at the 260-hPa level. The potential temperature along the trajectory increases by 2.6 K day^{-1}. The results of the tendency analysis confirm that in this part of the streamer diabatic processes govern the change in potential vorticity. At the steep frontal surface the rising of the warm air masses implies strong cloud formation. The release of latent heat in high convective clouds causes an increase in the vertical gradient of the heating rate and therefore an increase in potential vorticity.

To demonstrate the transport across the tropopause for all trajectories released at 0000 UTC 7 February the end points of these trajectories that crossed the 2-PVU surface downward (gray) and upward (black) are exhibited in Fig. 9. The results show downward transport in the region where the tropopause fold is deepest and upward transport at the eastern side of the fold in the area of the prefrontal cloudiness.

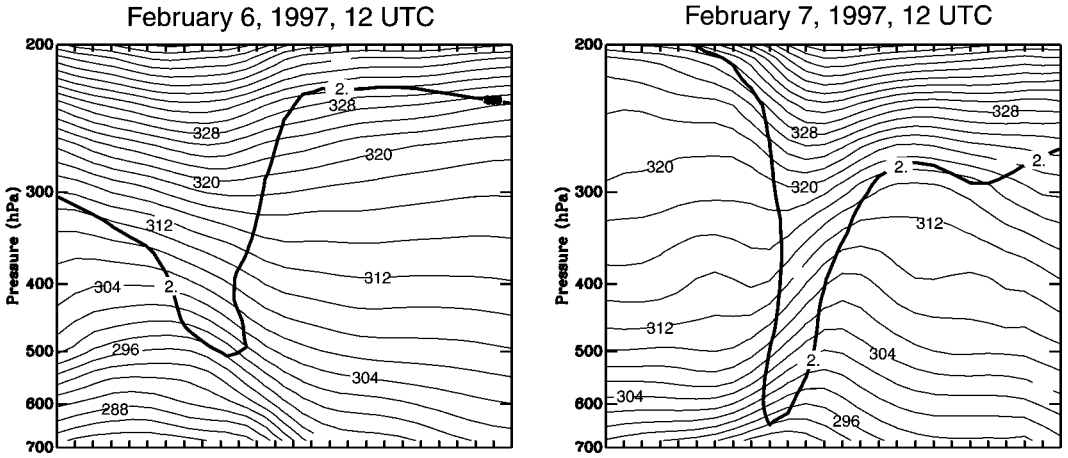

FIG. 6. Vertical cross sections of potential temperature (thin isolines) and of the 2-PVU surface (bold line) (left) at 1200 UTC 6 Feb 1997 and (right) at 1200 UTC 7 Feb 1997 along the lines marked in Fig. 3 (CS1 and CS2).

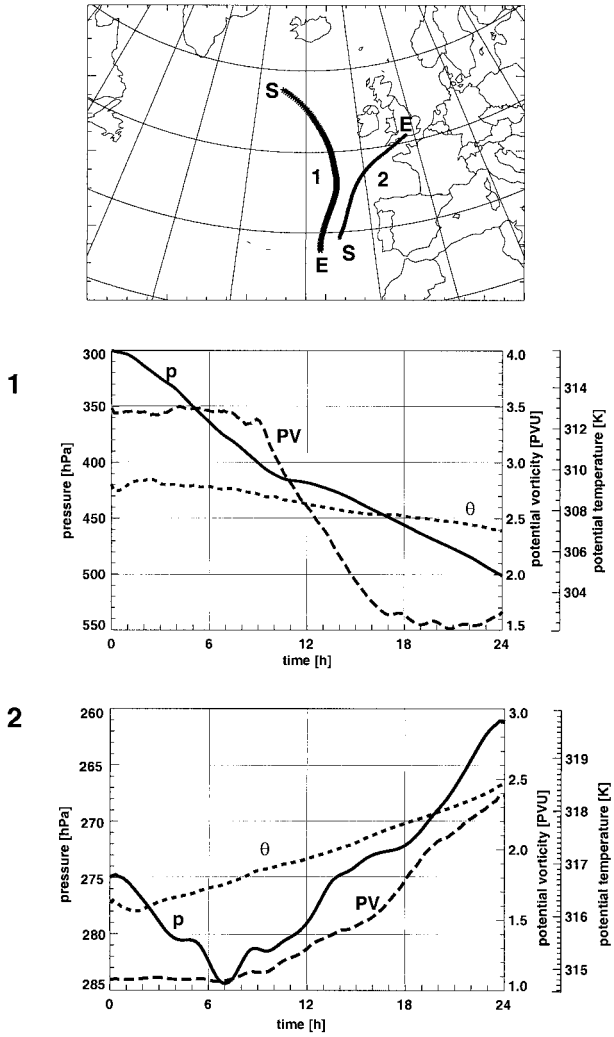

FIG. 7. Two examples of forward trajectories released at 0000 UTC 7 Feb at 300 hPa in the northwestern part of the box displayed in the lower panel of Fig. 2 (trajectory 1, black cross) and in the southern part (trajectory 2, white cross), respectively. (a) Horizontal displacements of the air parcels, S and E mark the start and end points of the trajectories; (b) vertical displacements of trajectory 1 in terms of pressure (p), PV, and potential temperature (θ); and (c) same as (b) but for trajectory 2.

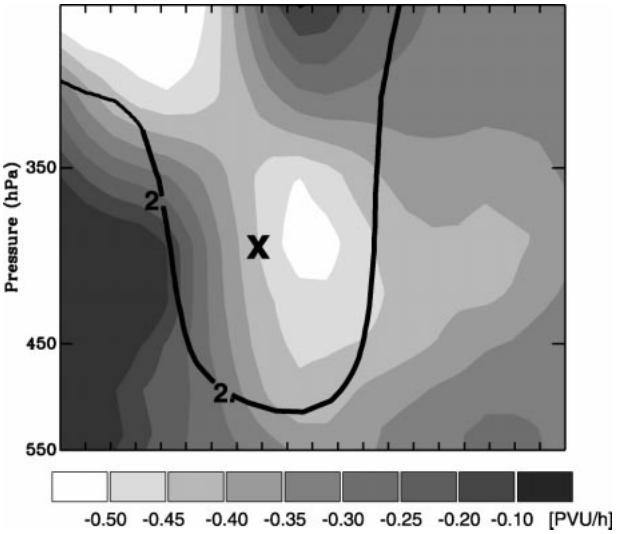

FIG. 8. Vertical cross section of the potential vorticity tendency due to diffusion (gray shading) and the 2-PVU surface (bold line) at 0900 UTC 7 Feb along 46°N. The cross marks the position of the trajectory at this time.

While similar processes have been recognized during the previous days (5 and 6 February), where turbulent diffusion governs the transport from the stratosphere into the troposphere the dynamical regime changes on 8 February. The streamer breaks up and the vortex that encloses the polar stratospheric air masses moves over the warm ocean at the west coast of North Africa (Fig. 4) where solar surface heating is stronger. This heat source and the destabilization of the lower troposphere due to the PV anomaly lead to convection. The Meteosat data as well as the clouds calculated by the MM5 (not shown here) confirm the existence of strong convection in the area of the cutoff low. In contrast to the previous days, the evolution of PV along trajectories released inside the cutoff low shows a decrease due to the decrease of the vertical gradient of potential temperature tendency.

b. Results from Wei's formula

The results of 24-h average fluxes as inferred from Wei's formula [(2)] are shown in Fig. 10 for 1200 UTC 7 February. The flow diagram displays a dipole pattern similar to the results of the trajectory analyses (Fig. 9), that is, strong downward fluxes in the region of the tropopause fold and upward fluxes at the eastern edge. The processes responsible for this pattern were described in the previous section. A strong dipole pattern

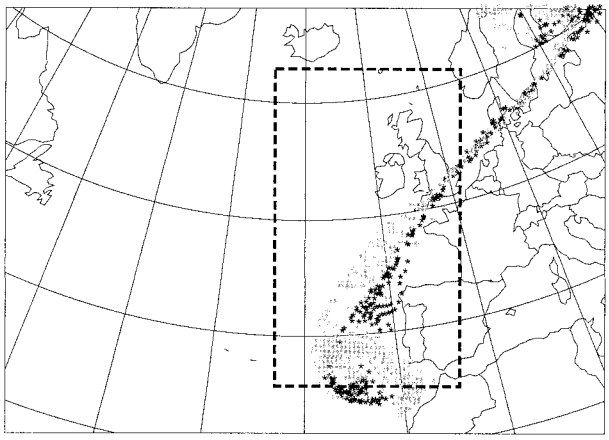

FIG. 9. Final points of tropopause crossing trajectories released inside the box as displayed in the lower panel of Fig 2 at 0000 UTC 7 Feb 1997. Downward fluxes through the 2-PVU surface are gray, upward fluxes black.

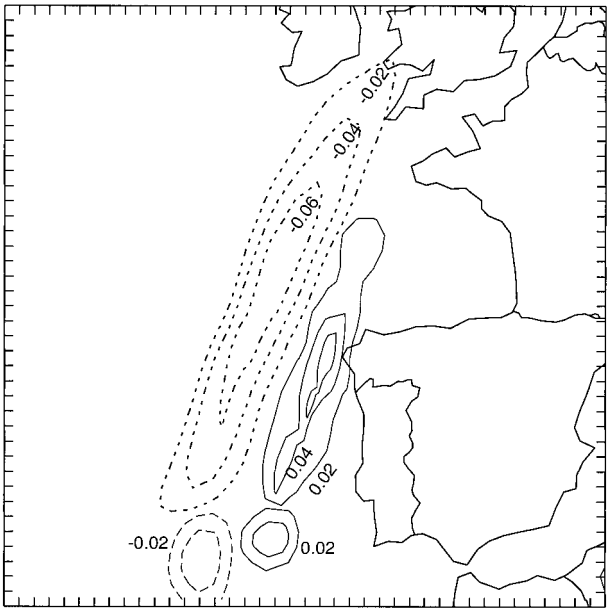

FIG. 10. Airmass fluxes across the 2-PVU surface (kg m^{-2} s^{-1}) calculated with Wei's formula at 1200 UTC 7 Feb. Dashed lines mark downward fluxes (from the stratosphere to the troposphere), solid lines upward fluxes (from the troposphere to the stratosphere).

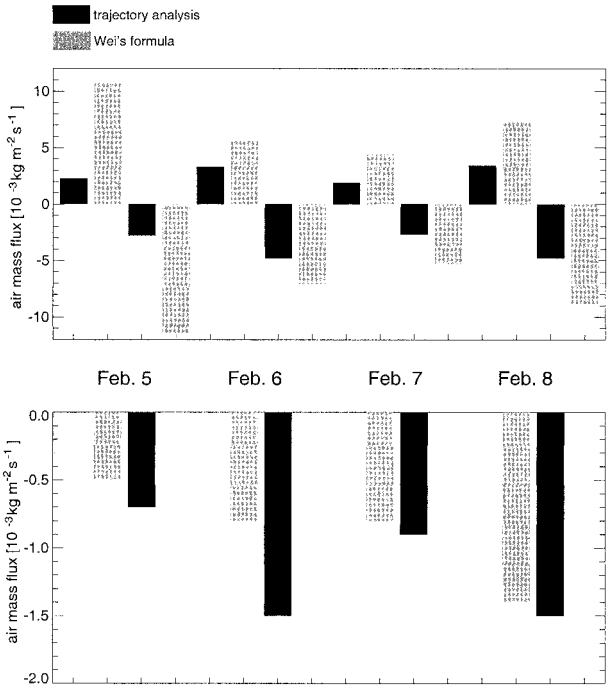

FIG. 11. Airmass fluxes across the 2-PVU surface as calculated with the trajectory method (black bars) and Wei's formula (gray bars) 5–8 Feb: (top) upward and downward fluxes and (bottom) net fluxes.

was also identified in Lamarque and Hess (1994), who also applied the method of Wei. This good agreement between the parcel picture and the flow diagram is also evident during the other analyzed days (5–8 February). The dipole pattern reflects the secondary cross-frontal circulation, the associated upwelling and downwelling of which is most prominently visible in terms of **Q** vectors (see, e.g., Keyser et al. 1992; Elbern et al. 1998).

c. Flux estimates and discussion of the methods

In order to quantify the airmass fluxes across the 2-PVU surface we analyzed the period from 0000 UTC 5 February to 0000 UTC 9 February, which was most interesting with regard to the tropopause dynamics. Figure 11 combines the results of the trajectory analysis and the application of Wei's formula. In the upper panel of Fig. 11 the upward and downward fluxes are displayed while the lower panel shows the net fluxes across the 2-PVU surface. For the entire episode the trajectory calculations show an average downward airmass transport across the 2-PVU surface of -1.0×10^{-3} kg m^{-2} s^{-1}. A similar result was obtained by applying Wei's formula. The average net flux of air masses amounts to -1.1×10^{-3} kg m^{-2} s^{-1}. The net flux values coincide well for the whole period analyzed. Differences occur between the amounts of upward and downward fluxes as calculated by the two methods. The results of the trajectory analysis amount to an average of about 50% of the values obtained by Wei's formula. A possible reason for this discrepancy is the different temporal resolution of both methods. Employing Wei's formula we calculate the airmass flux every hour. The trajectory method sums the mass of the parcels that cross the 2-PVU surface every 6 h. Therefore the second method is not able to resolve temporally all processes contributing to the exchange of air masses. Another, and probably more relevant, origin of the discrepancy between the absolute flux estimates may be introduced by the basic assumption made in Wei's formula—an auxiliary line is defined to avoid an ambiguous definition of the tropopause height by construction of single-valued PV columns (Fig. 1 in Wei 1987). In effect, in the course of the intrusion process, the stratosphere-to-troposphere transition process is formally calculated by attributing air mass passing this auxiliary line to the troposphere though it is really still in the stratosphere. In the case of irreversible mixing, the error induced by this assumption is negligible if the integration time of estimate is sufficiently long, say, days rather than hours. In the case of no mixing, when air masses in a fold are carried back into the stratosphere, Wei's formula compensates for this formally generated flux thus enabling realistic estimates of airmass fluxes over a sufficiently long time interval.

A further numerical problem already discussed by Lamarque and Hess (1994) and Wirth and Egger (1999) results from the parameterization of Wei's formula. Here small areas with very large values occur due to a diverging Jacobian in certain regions with no physical evidence for transport across the tropopause. This effect leads to an overestimation of upward and downward

TABLE 1. Airmass fluxes across the 2-PVU surface calculated applying the trajectory method for different case studies. Positive values indicate upward fluxes from the troposphere to the stratosphere, negative values indicate downward fluxes from the stratosphere to the troposphere.

Case study	Airmass fluxes (10^{-3} kg m^{-2} s^{-1})		
	Upward	Downward	Net
Cutoff low: (22–26 Oct 1993)	3.0	−3.8	−0.8
Trough/tropopause fold: 2–6 Mar 1995	2.6	−3.7	−0.9
Cutoff low (North Atlantic): 14–21 Jun 1996	1.6	−2.2	−0.6
Trough/cutoff low (Europe): 21–27 Jun 1996	0.8	−1.4	−0.6
Trough/streamer: 5–9 Feb 1997	2.4	−3.5	−1.1

fluxes. Despite such deficiencies the net fluxes show a clear agreement in terms of position and amplitude, which is remarkable since both methods are based on completely different principles.

The fluxes are in the same order of magnitude as calculated for other episodes where tropopause folds (e.g., Ebel et al. 1996) and cutoff lows (e.g., Ancellet et al. 1994) were studied (Table 2).

Considering the numerical and methodical differences between these two techniques, one may place more confidence in the soundness of the flux estimates due to the small variance of the results (Table 1), although the problem of the validation of these results against measurements still remains. The good agreement between the different methods emphasized their scientific equivalence and offers the option for a convenient choice. Trajectory analyses are needed to trace the evolution of air parcels and to investigate the relevance of diabatic and turbulent diffusive processes for the tendency of potential vorticity along the pathways trough the tropopause. The application of Wei's formula provides insight into the same quantities from an Eulerian viewpoint.

Several sensitivity studies were carried out for both methods concerning the horizontal and vertical resolution of the underlying model, the application of different PV surfaces for the definition of the tropopause, and the amount of turbulent diffusion. The application of coarser horizontal resolutions (>50 km) yields stronger downward fluxes across the tropopause in particular with Wei's method. However, these results seem to be less plausible when comparing the temporal evolution of the flux values with the evolution of the tropopause fold. This is not surprising as with a coarser horizontal resolution the model is not able to properly resolve the observed mesoscale features (Ravetta et al. 1999). The usage of a higher vertical resolution yields no considerable differences in the flux estimates. Both methods coincidently reveal a decrease of airmass fluxes with an increasing value of potential vorticity. Doubling and halving the variation of the diffusion coefficient revealed no significant differences of the resulting flux estimates. After two days of simulation the difference remains lower than 5%. However, until now a validation of the turbulence schemes was not possible. Systematic studies of stratosphere–troposphere exchange (STE)—both numerically (e.g., Lamarque and Hess 1994) and by direct airborne measurements (e.g., Shapiro 1980)—confirm the relevance of this parameter for the STE. Therefore a comparison of different numerical schemes and validation against measurements will be unavoidable in the future.

4. Flux estimates for different meteorological situations

For the study of cross-tropopause airmass fluxes occurring in different meteorological situations the trajectory method was employed. This choice was motivated by the desire to identify the processes responsible for an estimated change in potential vorticity of air masses crossing the tropopause. As argued in the previous section the trajectory-based analysis is the most convenient one for this purpose.

Until now we analyzed five case studies in detail looking especially at tropopause folds, cutoff lows, and streamers. Table 1 summarizes the results obtained for

1) a cutoff low over central Europe in October 1993 (Kowol-Santen 1998);
2) an upper-level trough and associated tropopause fold over central Europe in March 1995 (the Transport of Ozone and Stratosphere–Troposphere Exchange program (TOASTE-B) campaign], as described in detail by Ravetta et al. (1999);
3) a cutoff low that moved over the North Atlantic eastward and decayed over Europe during June 1996 (TOASTE-C campaign) as described by Gouget et al. (2000);
4) a trough and cutoff low over central Europe in June 1996 [TOASTE-C campaign; Kowol-Santen (1998)]; and
5) the streamer described in section 3.

A net downward airmass flux across the tropopause was obtained for all listed cases. The fluxes are strongest for the streamer in February 1997 where on an average 9×10^{14} kg of air was transported per day from the stratosphere into the troposphere. The lowest flux values occurred for the cutoff low over central Europe in June 1996 ($\sim 5.8 \times 10^{-3}$ kg m^{-2} s^{-1}). Values only about 10% larger were found for the cutoff low over the Atlantic during the same month.

TABLE 2. Values of airmass fluxes across the tropopause published in the literature. Negative values indicate transport from the stratosphere in the troposphere.

Author (case study)	Time period (days)	Area (km^2)	Airmass exchange (10^{14} kg)	Airmass fluxes (10^{-3} kg m^{-2} s^{-1})
Lamarque and Hess (1994) (tropopause fold)	4	3.2×10^6	4.9	−0.4
Spaete et al. (1994) (tropopause fold)	1	10^6	3.0	−3.5
Vaughan et al. (1994) (tropopause fold)	2	2.6×10^5	1.1	−2.4
Wirth (1995) (cutoff low)	3	8.0×10^5	7.2	−3.5
Ebel et al. (1996) (tropopause fold)	1.96	2.25×10^6	5.4	−1.4

The comparison of the downward and upward fluxes shows that they differ by less than 15% for the three case studies in autumn and winter, whereas for the summer cases investigated they amount to only one-third to two-thirds of the autumn and winter values, respectively. The ratios of up- to downgoing fluxes amount to about 3:4 for the autumn cutoff low and the cutoff low over the Atlantic in June, and to about 2:3 for the winter case studies and the summer cutoff low over central Europe. The largest net downward transport in the region of the streamer occurred due to the deepest enfolding of the tropopause during this time period and the coupling of the fold to a cold front with strong downward winds and vertical shear (see previous sections). Similar but slightly weaker processes were simulated for the trough and tropopause fold in March 1995 (Kowol-Santen 1998; Ravetta et al. 1999).

For the cutoff low in October 1993 the flux calculations yield in certain areas larger amounts of tropospheric air transported into the stratosphere. This is due to radiative heating at the top of high cirrus clouds located in the southeastern part of the analyzed area, which is associated with an increase in the vertical gradient of potential temperature tendency and causes a gain in potential vorticity (Kowol-Santen 1998). This results in lower net fluxes than obtained for the streamer and trough case (Table 1).

The three-dimensional trajectory analysis reveals two main processes responsible for the decay of the cutoff low moving eastward over the Atlantic in June 1996. At the outer layers thin filaments developed, which were stretched along the flank of the jet stream. This dynamical process agrees with results presented by Gouget et al. (2000). The authors compared results of trajectory calculations to Measurement of Ozone and Weather Vapor by Airbus In-Service Aircraft measurements, which also show these filamentation processes. Some of the filaments broke up and were mixed into the troposphere. In these regions the model results exhibit strong turbulent processes with lateral mixing of potential vorticity. At the same time smaller filaments of tropospheric air penetrated into the lower part of the cutoff low between 350 and 400 hPa. Slight convection affected the base of the cutoff low on 17 and 18 June, which weakened during the following day and set in again on 20 June when the cutoff low was situated over the Bay of Biscay. The net flux amounts—similar to the upward and downward fluxes—were nearly 60% of the values estimated for the winter cases.

The episodes described above were mainly influenced by turbulent diffusion due to strong vertical wind shear at the frontal systems. By contrast diabatic processes dominated during the summer episode over central Europe. As pointed out in Ravetta and Ancellet (2000) strong convective activity was responsible for the decay of the cutoff low. The associated exchange of air between the lower stratosphere and the upper and middle troposphere was much weaker as indicated by the calculated upward and downward fluxes (Table 1). The net flux was of the same order of magnitude as obtained for the cutoff low over the Atlantic.

Table 2 summarizes the results of airmass fluxes published in the literature. The results for all case studies range between the estimate obtained by Lamarque and Hess (1994) of 4.9×10^{14} kg (4 days)$^{-1}$ (3.2×10^6 km^2)$^{-1}$ (which corresponds to 4.4×10^{-4} kg m^{-2} s^{-1}) and Ebel et al. (1996) of 5.4×10^{14} kg (1.96 days)$^{-1}$ (2.25×10^6 km^2)$^{-1}$ (which corresponds to 1.4×10^{-3} kg m^{-2} s^{-1}). Both studies apply the formula of Wei for meteorological fields simulated with the MM4 and MM5. However, one should be aware of the different spatial and temporal resolutions used when comparing the results. Lamarque and Hess (1994) discuss a case where diabatic processes were responsible for the transport across the tropopause, whereas Ebel et al. (1996) look at an episode with a very deep tropopause fold when diabatic effects were negligible for the change of potential vorticity which was mainly caused by turbulent diffusion. In accordance with the studies by Lamarque and Hess (1994) and Ebel et al. (1996) the results of the present analysis also suggest that in regimes where the exchange is dominated by diabatic processes the net fluxes are smaller than in the case when the contribution from diffusive processes prevails.

Notably higher flux values were estimated by Spaete et al. (1994) analyzing a tropopause fold and by Vaughan et al. (1994) investigating a cutoff low. These studies yielded net downward flux values of 3.5×10^{-3} kg m^{-2} s^{-1} and 2.4×10^{-3} kg m^{-2} s^{-1}, respectively. In addition to the fact that again different episodes were investigated, the applied methods differ. Spaete et al. (1994) used a model with the top at 100 hPa. This could lead to an underestimation of the upward fluxes as shown by Meyer (1997). Vaughan et al. (1994) only

discuss the stratosphere-to-troposphere transport for a cutoff low in October 1990. Therefore their estimate should be compared to our downward flux values. It lies between the estimates for the cutoff low in June 1996 over the Atlantic and the cutoff low in October 1993 (Table 1). The flux estimates in the present study were checked applying two different methods. The results differ by less than 10% for a single selected episode. The estimates for different meteorological situations were carried out using a single method to generate comparable results. We emphasize that it is the first time that homogeneously derived results for cross-tropopause fluxes become available that occur under varying meteorological conditions.

5. Conclusions

The episodic airmass exchange across the tropopause given in the literature differs greatly. This study provides an elaborate comparison of different analysis methods as well as different meteorological situations. The comparative analysis allowed us to clarify the origin of the variability of the published estimates. The first part of the paper features two different analysis tools for the flux estimates, that is, the formula of Wei and a trajectory-based analysis. Both were implemented into the EURAD model system and applied for a case study in February 1997. The comparison of the results shows a remarkably good agreement of net downward flux estimates between both methods. Differences occurred between the upward and downward flux estimates. These discrepancies can be attributed to different numerical treatments of transport—Eulerian versus Lagrangian—as well as to the use of different temporal resolution and the different definition of the exchange interval as discussed in section 3c. In contrast the calculated net fluxes deviated by less than 10% on average.

The agreement between the two completely different methods may be taken as confirmation of the soundness of the flux estimates. However, since the stratospheric–tropospheric exchange fluxes are not amenable to direct measurement, the comparison of different numerical approaches, each of which with its specific advantages and weakness, it is a pertinent way to improve the precision of cross-tropopause transport estimates. Potential sources of errors, for example, the conservation of mass along trajectories or the tropopause definition within the parameterization of Wei's formula, may degrade the results.

In the second step different meteorological situations were investigated using one method in order to establish a broader database for the discussion of transport across the tropopause. One of the often discussed and not yet fully clarified questions concerns the processes responsible for the transport across the tropopause. As the trajectory-based analysis allows for explicitly distinguishing between the contribution of turbulence and diabatic processes when looking at the change in potential vorticity and following the movement of air parcels, this method was selected for the estimation of cross-tropopause fluxes under different meteorological conditions. In this way a broader basis of flux data derived in a homogeneous way could be established.

Three cutoff low events, an upper-level trough with associated tropopause fold, and a streamer case were investigated in detail using the EURAD model system (Table 1). The largest fluxes occurred in the region of the streamer related to a quite deep tropopause folding amounting to 1.0×10^{-3} kg m^{-2} s^{-1}. The smallest fluxes were computed for the cutoff low over Europe in June 1996 (5.8×10^{-4} kg m^{-2} s^{-1}). The analysis of the PV budget along the trajectories showed that during most of the autumn and winter episodes the exchange was determined by turbulence and associated mixing. Diabatic effects are more important during the summer episodes and appear to be responsible for the erosion of the cutoff lows over Europe. They also dominated the transport across the tropopause as a consequence of strong convection in the cutoff low that developed at the tip of the streamer in February 1997. These results exhibit that diabatic processes associated with convection are dominating the transport across the tropopause over land in summer and over warm seas in winter in agreement with the findings of Price and Vaughan (1993).

Five case studies are still not sufficient to arrive at final statements about the seasonally and dynamically controlled variation of cross-tropopause fluxes. In summary, simulated episodes in this study show that larger flux values apparently occur for streamers and tropopause folds in winter in contrast to cutoff lows in summer. This is in agreement with the results obtained by, for example, Danielsen and Mohnen (1977), Austin and Follows (1991), and Gettelman and Sobel (2000), who give an additional hint that exchange processes observed in the winter/spring period are stronger compared to the summer months. The findings of Price and Vaughan (1993) support this result.

Four items deserve further investigation. First, sensitivity studies according the influence of numerical parameterizations on the flux estimates should be carried out. The validation of the diffusion schemes applied would be important. Furthermore, subgrid-scale processes are not parameterized in our tools. They are essential for the estimation of convective fluxes and particularly important for cutoff lows. Third, the role of spatial and temporal resolution of the models should be investigated in more detail. Fourth, it is necessary to analyze more case studies applying one method in order to achieve statistically significant results and to judge whether there is a seasonally and dynamically dependent variation of the transport across the tropopause.

Acknowledgments. The authors are grateful to two anonymous reviewers for helpful comments. Many thanks are also due to Dr. Raimund Meyer, Institute for

Geophysics and Meteorology, Cologne, Germany, for providing the MM5 version with flux calculation software. This work has been supported by the European Commission under the TOASTE-C program. We are grateful to Institutes 2 and 3 for Chemistry and Geodynamics and the Central Institute for Applied Mathematics of the Research Centre Jülich for giving computational support. We thank the ECMWF and the German Weather Service for the permission to use extracts of their global meteorological dataset.

REFERENCES

Ancellet G., J. Pelon, M. Beekmann, A. Papayannis, and G. Megie, 1991: Ground-based lidar studies of ozone exchanges between the stratosphere and the troposphere. *J. Geophys. Res.,* **96,** 22 401–22 421.

——, M. Beekmann, and A. Papayannis, 1994: Impact of a cutoff low development on downward transport of ozone in the troposphere. *J. Geophys. Res.,* **99,** 3451–3468.

Austin, J. F., and M. J. Follows, 1991: The ozone record at Payerne: An assessment of the cross-tropopause flux. *Atmos. Environ.,* **25A,** 1873–1880.

Blackadar, A. K., 1979: High resolution models of the planetary boundary layer. *Advances in Environmental Science and Engineering,* J. Pfafflin and E. Ziegler, Eds., Vol. 1, Gordon and Breach, 3–49.

Danielsen, E. F., and V. A. Mohnen, 1977: Project Dustorm Report: Ozone transport, in situ measurements, and meteorological analyzes of tropopause folding. *J. Geophys. Res.,* **82,** 5867–5877.

Ebel, A., H. Hass, H. J. Jakobs, M. Memmesheimer, M. Laube, A. Oberreuter, H. Geiss, and Y.-H. Kuo, 1991: Simulation of ozone intrusion caused by a tropopause fold and cut-off low. *Atmos. Environ.,* **25A,** 2131–2144.

——, H. Elbern, J. Hendricks, and R. Meyer, 1996: Stratosphere–troposphere exchange and its impact on the structure of the lower stratosphere. *J. Geomag. Geoelectr.,* **48,** 135–144.

Elbern, H., J. Kowol, R. Sladkovic, and A. Ebel, 1997: Deep stratospheric intrusions: A statistical assessment with model guided analyzes. *Atmos. Environ.,* **31,** 3207–3226.

——, J. Hendricks, and A. Ebel, 1998: A climatology of tropopause folds by global analyses. *Theor. Appl. Climatol.,* **59,** 181–200.

Gettelman, A., and A. H. Sobel, 2000: Direct diagnoses of stratosphere–troposphere exchange. *J. Atmos. Sci.,* **57,** 3–16.

Gouget, H., G. Vaughan, A. Marenco, and H. G. J. Smit, 2000: Decay of a cut-off low and contribution to stratosphere–troposphere exchange. *Quart. J. Roy. Meteor. Soc.,* in press.

Grell, A. G., J. Dudhia, and D. R. Stauffer, 1993: A description of the fifth-generation Penn State/NCAR Mesoscale Model (MM5). NCAR Tech. Note. NCAR/TN−398 + 1A, 122 pp. [Available online at ftp://ftp.ucar.edu/mesouser/Documents.]

Grewe, V., and M. Dameris, 1996: Calculating the global mass exchange between stratosphere and troposphere. *Ann. Geophys.,* **14,** 431–442.

Hoerling, M. P., T. K. Schaack, and A. L. Lenzen, 1993: A global analysis of stratospheric–tropospheric exchange during northern winter. *Mon. Wea. Rev.,* **121,** 162–172.

Keyser, D., B. Schmidt, and D. Duffy, 1992: Quasigeostrophic vertical motions diagnosed from along- and cross-isentrope components of the Q-vector. *Mon. Wea. Rev.,* **120,** 731–741.

Kowol-Santen, J., 1998: Numerische Analysen von Transport- und Austausch prozessen in der Tropopausenregion der mittleren Breiten. Ph.D. thesis, Mitteilungen aus dem Institut für Geophysik und Meteorologie der Universität zu Köln, 186 pp. [Available from jr@eurad.uni-koeln.de.]

Kuo, H. L., 1974: Further studies of the parameterization of the influence of cumulus convection on large-scale flow. *J. Atmos. Sci.,* **31,** 1232–1240.

Lamarque, J.-F., and P. G. Hess, 1994: Cross-tropopause mass exchange and potential vorticity budget in a simulated tropopause folding. *J. Atmos. Sci.,* **51,** 2246–2269.

Meyer, R., 1997: Quantitative Analysen von Luftmassenflüssen durch die Tropopause in mittleren Breiten mit einem mesoskaligen meteorologischen Modell. Ph.D. thesis, Mitteilungen aus dem Institut für Geophysik und Meteorologie der Universität zu Köln, 153 pp. [Available from jr@eurad.uni-koeln.de.]

Pedlosky, J., 1979: *Geophysical Fluid Dynamics.* Springer-Verlag, 310 pp.

Price, J. D., and G. Vaughan, 1993: On the potential for stratosphere–troposphere exchange in cut-off low systems. *Quart. J. Roy. Meteor. Soc.,* **119,** 343–365.

Ravetta, F., and G. Ancellet, 2000: Identification of dynamical processes at the tropopause during the decay of a cutoff low using high-resolution airborne lidar ozone measurements. *Mon. Wea. Rev.,* **128,** 3252–3267.

——, ——, J. Kowol-Santen, R. Wilson, and D. Nedeljkovic, 1999: Ozone, temperature, and wind field measurements in a tropopause fold: Comparison with a mesoscale model simulation. *Mon. Wea. Rev.,* **127,** 2641–2653.

Shapiro, M. A., 1980: Turbulent mixing within tropopause folds as a mechanism for the exchange of chemical constituents between the stratosphere and the troposphere. *J. Atmos. Sci.,* **37,** 994–1004.

Spaete, P., D. R. Johnson, and T. K. Schaack, 1994: Stratospheric–tropospheric mass exchange during the Presidents' Day Storm. *Mon. Wea. Rev.,* **122,** 424–439.

Vaughan, G., J. D. Price, and A. Howells, 1994: Transport into the troposphere in a tropopause fold. *Quart. J. Roy. Meteor. Soc.,* **120,** 1085–1103.

Wei, M.-Y., 1987: A new formulation of the exchange of mass and trace constituents between the stratosphere and troposphere. *J. Atmos. Sci.,* **20,** 3079–3086.

Wirth, V., 1995: Diabatic heating in an axisymmetric cut-off cyclone and related stratospheric–tropospheric exchange. *Quart. J. Roy. Meteor. Soc.,* **121,** 127–147.

——, and J. Egger, 1999: Diagnosing extratropical synoptic-scale stratosphere–troposphere exchange: A case study. *Quart. J. Roy. Meteor. Soc.,* **125,** 635–655.